# Knockout of the HCC suppressor gene Lass2 downregulates the expression level of miR-694

XIAODONG LU[1,2], YUANYUAN CHEN[2], TIANTIAN ZENG[2], LUFANG CHEN[2], QIXIANG SHAO[2] and WENXIN QIN[1]

[1]State Key Laboratory of Oncogenes and Related Genes, Shanghai Cancer Institute, Shanghai 200032; [2]School of Medical Science and Laboratory Medicine, Jiangsu University, Zhenjiang, Jiangsu 212013, P.R. China

Received July 14, 2014; Accepted September 2, 2014

DOI: 10.3892/or.2014.3527

**Abstract.** *Homo sapiens* longevity assurance homolog 2 of yeast LAG (Lass2) catalyzes the synthesis of long-chain ceramide which is an essential element of membranous structures. Deletion of Lass2 is associated with a high risk of spontaneous or DEN-induced hepatocellular carcinoma (HCC), yet the mechanism remains unclear. In the present study, we found extensive vesicles in hepatocytes of one-month-old Lass2-knockout (KO) mice. Hepatic biochemical indices were increased and expression of albumin was attenuated in the one-month Lass2-KO liver. The results indicate that the injuries of the hepatocytes in young Lass2-KO mice, based on the results of Gene Ontology analysis of mRNA microarray of Lass2-KO liver vs. wild-type liver showed 'wounding response' was the mostly possible altered pathway in the Lass2-KO mice. miR-mRNA integrated analysis revealed that miR-694 was downregulated while its target gene tumor necrosis factor α-induced protein 3 (Tnfaip3) was upregulated, as confirmed by qPCR. The expression of NF-κB which is negatively controlled by Tnfaip3 was detected by qPCR and was found to be downregulated. Herein, we first report that Lass2 deficiency caused the downregulation of miR-694 and the upregulation of its target gene Tnfaip3 *in vivo* in mice, which may be related to a high risk of occurrence of HCC.

*Correspondence to:* Professor Xiaodong Lu, State Key Laboratory of Oncogenes and Related Genes, Shanghai Cancer Institute, 25/Ln 2200 Xie-Tu Road, Shanghai 200032, P.R. China
E-mail: lu_xdg@hotmail.com

Professor Qixiang Shao, School of Medical Science and Laboratory Medicine, Jiangsu University, 301 Xue-Fu Road, Zhenjiang, Jiangsu 212013, P.R. China
E-mail: shao_qx@ujs.edu.cn

*Abbreviations:* Lass2, longevity assurance gene 2; KO, knockout; miR or miRNA, microRNA; Tnfaip3, tumor necrosis factor α-induced protein 3; NF-κB, nuclear transcription factor-κB; qPCR, real-time quantitative PCR; HCC, hepatocellular carcinoma

*Key words:* Lass2, miR-694, Tnfaip3, NF-κB

## Introduction

Recently *Homo sapiens* longevity assurance homolog 2 of yeast LAG (Lass2) has attracted the interest of researchers since a large amount of evidence has demonstrated that Lass2 is a potential tumor-suppressor gene. Deficiency of Lass2 is involved in the tumorigenesis of various types of tumors, especially hepatocellular carcinoma (HCC) (1-4). It has been reported that two of three non-specific Lass2-deleted mice presented liver cancer spontaneously when they were about nine months old (3). In our recently published study, using a hepatocellular-specific Lass2-knockout (KO) animal model, we found that Lass2-KO mice were more susceptible to the carcinogen DEN, i.e., DEN caused the Lass2-KO mice to develop liver tumors earlier and the tumors developed more rapidly (5).

To explore the biological functions of Lass2 and the related mechanisms it employs to suppress HCC, the structures and functions of the livers of the Lass2-KO mice and wild-type (WT) mice were compared. Meanwhile, microarrays of mRNAs and miRNAs of the livers from the two genotypes were performed and analyzed.

## Materials and methods

*Animals*. The hepatocyte-specific Lass2-KO mice used in the present study were generated by the crossing of mice (C57BL/6J) carrying floxed the second exon of Lass2 and Albumin-Cre transgenic mice (C57BL/6J), as previously reported (5). All protocols for animal care and use were approved by the Regulations for the Administration of Affairs Concerning Experimental Animals (The State Science and Technology Commission of P.R. China, 1988), and the Animal Experimental Center of Jiangsu University was licensed for animal experiments. All of the mice were housed in pathogen-free (SPF) animal facilities under a standard 12-h-light/12-h-dark cycle. Animals received free access to water and commercial mouse chow throughout the present study. One-month-old male Lass2-KO and -WT mice were sacrificed by cervical dislocation. The mice for the experiments

that followed were n=10/group. Liver weight/body weight were measured.

*Biochemical estimation*. The mice were sacrificed by cervical dislocation, and blood harvested from the inferior vena cava was centrifuged at 1,600 x g for 10 min at room temperature to obtain serum for hepatic biochemical estimation. The activities of aspartate aminotransferase (AST), alanine aminotransferase (ALT) and lactate dehydrogenase (LDH) in serum were estimated using an AutoAnalyzer (Hitachi 7600, Japan) at the Affiliated Hospital of Jiangsu University.

*Histological sections and staining*. Liver tissues were immediately removed from the sacrificed mice, partly fixed in AAF (100% alcohol 85 ml, acetic acid 5 ml, formalin 10 ml) for morphological examination, and partly stored at -80˚C for further use. The tissues were paraffin-embedded and sectioned (5-$\mu$m thick). Periodic acid-Schiff (PAS) staining was performed using a commercially available kit (cat. no. 0609A14; Shellfish Gamma Biotechnology Co., Ltd., Nanjing, China). Briefly, the sections were incubated in 0.5% periodic acid solution for 15 min, rinsed with distilled water, and exposed to Schiff's reagent for 20 min followed by two 3-min exposures to 0.6% sodium metabisulfite.

*Western blotting*. Tissues were lysed in RIPA lysis buffer containing the protease inhibitor phenylmethanesulfonyl fluoride (cat. nos. P0013C and ST506; both from Beyotime Institute of Biotechnology). The cell extracts were centrifuged at 12,000 x g for 20 min at 4˚C in a Beckman Avanti-30 centrifuge, and the supernatants were used for the experiments. The protein concentrations were determined with the BCA assay kit (cat. no. P0009; Beyotime Institute of Biotechnology). The equivalent tissue proteins (10 $\mu$g/lane) were subjected to electrophoresis on a Mini-Protean Tetra Electrophoresis System (165-8001; Bio-Rad, Hercules, CA, USA) and transferred onto PVDF membranes (Millipore, Bedford, MA, USA) via a semi-dry transfer system (Bio-Rad). The membranes were blocked with 5% non-fat milk for 1 h at room temperature in TBST [50 mM (pH 7.5) Tris, 0.9% NaCl and 0.1% Tween-20] and then incubated with a 1:200 dilution of rabbit anti-mouse/human albumin (cat. no. BS6520; Bioworld Technology, Inc., Dublin, OH, USA) overnight at 4˚C. The membranes were washed and then incubated with peroxidase goat anti-rabbit antibody (cat. no. XR-9920; ProSci Inc., Poway, CA USA) for 1 h at room temperature and developed using the BeyoEcl Plus kit (cat. no. P0018; Beyotime Institute of Biotechnology) for 1 min, and then scanned by ChampChemi professional (SG2011; Beijing Sage Creation Science Co., Ltd., Beijing, China).

*RNA isolation and qPCR analysis*. Total RNA including miRNA from liver tissues was extracted by TRIzol (cat. no. 15596026; Invitrogen Corp., Carlsbad, CA, USA) or the miRNeasy Mini kit (cat. no. 217004; Qiagen, Hilden, Germany) according to the manufacturer's suggestions. For mRNA qPCR, RNA was transcribed into cDNA using the QuantiTect reverse transcription kit and QuantiTect SYBR-Green PCR kits (cat. no. 205311 and no. 204243; both from Qiagen) according to the manufacturer's protocols. For miRNA qPCR, RNA was transcribed into cDNA using the miScript Reverse II transcription kit (cat. no. 218161; Qiagen). The reaction component consisted of total RNA 1 $\mu$g, miScript HiSpec buffer 4 $\mu$l, Nucleics Mix 2 $\mu$l, miScript reverse transcriptase mix 2 $\mu$l, RNase-free $H_2O$ up to 20 $\mu$l. The reaction was carried out at 37˚C for 60 min and 95˚C for 5 min on the ABI PCR 9700 system (Applied Biosystems, Foster City, CA, USA). cDNA was diluted in 80 $\mu$l nuclease-free $H_2O$ for further application by LightCycler 480 SYBR-Green I master (Roche, Switzerland; cat. no. 04887352001). The reaction system for qPCR consisted of: LightCycler 480 SYBR-Green I Master 5 $\mu$l, forward primer 0.2 $\mu$l, reverse primer 0.2 $\mu$l, cDNA 1 $\mu$l, nuclease-free $H_2O$ 3.6 $\mu$l. PCR was run on ABI 7500 Fast (Applied Biosystems) and normalized against the expression of GAPDH or U6. The program was performed at 95˚C for 10 min, 95˚C for 10 sec plus 60˚C for 30 sec for 40 cycles. For the melting curve evaluation, the temperature was slowly increased from 60˚C to 97˚C, and 5 acquisitions per ˚C were performed continuously. All samples were analyzed in triplicate. Relative expression was calculated using the comparative threshold cycle (Ct) method and was indicated as n-fold change = $-(\Delta Ct_{KO} - \Delta Ct_{WT})$. The primers for Tnfaip3, NF-κB and GAPDH were: for Tnfaip3, 5'-CAGCACCTAAG CCAACGAGT-3' and 5'-TGGACCTGTCAATGTGTTCG-3'; for NF-κB, 5'-AGCTTATGCCGAACTTCTCG-3' and 5'-GAC TCCGGGATGGAATGTAA-3'; for GAPDH, 5'-GCAAGG TCATCCCAGAG-3' and 5'-AAGTCGCAGGAGACAAC-3'; for miR-694 and U6, the miRNA specific primers were respectively: 5'-CTGAAAATGTTGCCTGAAG-3' and 5'-CAAGG ATGACACGCAAATTCG-3', whereas the reverse primer was the manufacturer-provided miScript universal primer.

*Microarrays of mRNA and miRNA*. Liver tissues from 2 one-month male Lass2-KO mice and 2 one-month male WT mice were respectively subjected to the experiments of Mouse OneArray (MOA 2.0 ver.) and Mouse and Rat miRNA OneArray (MRmiOA 4.0 ver.) using Phalanx microarray platform by Oebiotech Co. (Shanghai, China). Briefly, RNA was extracted from liver tissues with TRIzol reagent (Invitrogen), whose quantity and purity were assessed using a NanoDrop ND-1000 spectrophotometer (NanoDrop Technologies Inc., Wilmington, DE, USA). The purity and integrity of each extracted RNA met the requirements: $A_{260}/A_{280}$ >1.6, $A_{260}/A_{230}$ >1 and RNA integrity number (RIN) value >5. Small RNA fraction indicated the abundance of RNA <200 nt compared with the overall RNA area from Agilent RNA 6000 Nano assay and was acceptable for the miRNA assay. Possibility of genomic DNA contamination was excluded by gel electrophoresis. Two micrograms of RNA from each group was respectively converted into cyanine-5 labeled target cRNA, hybridized to either Mouse OneArray or Mouse and Rat miRNA OneArray by the Affymetrix GeneChip fluidics station 450, and scanned with an Affymetrix GeneChip scanner 3000 7G. After normalization, differentially expressed mRNAs or miRNAs were established at $\log_2$ |Fold change| >1 and P<0.05.

For advanced data analysis, all biological replicates were pooled and calculated to identify differentially expressed genes based on the threshold of fold change and the P-value. The correlation of expression profiles between biological replicates and treatment conditions was demonstrated by

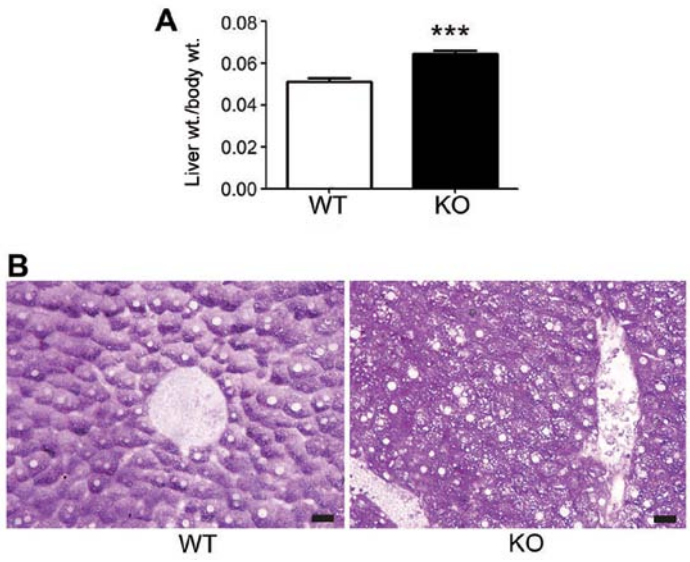


Figure 1. Representative image of structural alterations in the liver tissues from a hepatocyte-specific Lass2-KO mouse. (A) The average ratio of the liver weight/body weight of the Lass2-KO mice was higher than this ratio in the control WT mice. (B) Compared to the liver tissues from the WT mice, hepatocytes of the Lass2-KO displayed abundant vesicles. Scale bar, 20 $\mu$m. WT, wild-type; KO knockout. $^{***}$P≤0.001.

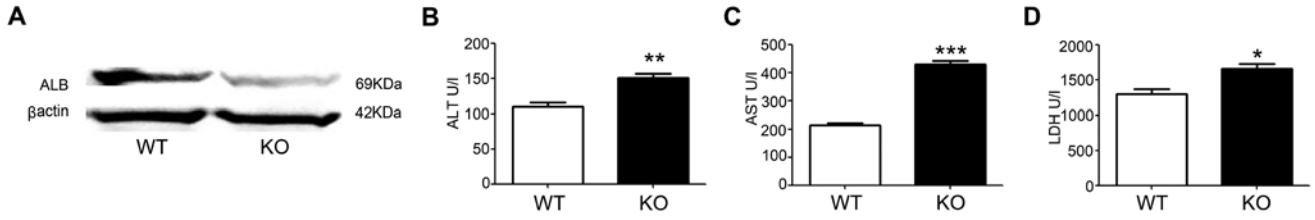


Figure 2. Alterations in the liver function of hepatocyte-specific Lass2-KO mice. (A) Expression of ALB was attenuated in the Lass2-KO mice. Levels of (B) ALT, (C) AST and (D) LDH in serum were respectively elevated in the Lass2-KO mice. $^{*}$P<0.05, $^{**}$P≤0.01 and $^{***}$P≤0.001.

unsupervised hierarchical clustering analysis. A subset of genes was selected for clustering analysis. An intensity filter was used to select genes where the difference between the maximum and minimum intensity values exceeded 4,000 among all microarrays. For this microarray project, the number of genes clustered was 272 genes. According to previously selected differentially expressed gene lists, Gene Ontology (GO) analysis was performed by Oebiotech Co. Targetscan 5.1 was utilized to predict miR-targeting mRNA. mRNA-miRNA integration analysis demonstrated potential mRNA targets with inverse expression alterations as their regulatory miRs displayed in the mRNA microarray or miRNA microarray.

*Statistical analysis*. Data were analyzed by the Student's t-test. P<0.05 was considered to indicate a statistically significant difference, and P≤0.01 and P≤0.001 are indicated by relevant symbols in the figures and legends. qPCR and western blot analyses were repeated three times.

## Results

*Structural alterations in the liver tissues from hepatocyte-specific Lass2-KO mice were noted in the PAS-stained sections*. The average ratio of liver weight/body weight of the Lass2-KO mice was higher than the ratio in the control WT mice (Fig. 1A). Compared to the liver tissues from the WT mice, the hepatocytes of the Lass2-KO displayed abundant vesicles (Fig. 1B).

*Liver functions and the expression of ALB are altered in Lass2-KO mice compared with the WT control*. The production of ALB in the liver was attenuated in the Lass2-KO mice (Fig. 2A). The levels of ALT, AST and LDH in serum were respectively elevated in the Lass2-KO mice, indicating abnormal liver function in the Lass2-KO mice (Fig. 2B-D), in accordance with the structural injury of the Lass2-KO hepatocytes.

*Profiles of mRNAs and miRNAs in the liver tissues are respectively reprogrammed in Lass2-KO mice vs. WT control*. mRNA and miRNA microarray results showed that over 600 mRNA were markedly upregulated and over 700 genes were downregulated; whereas 13 miRNAs were markedly upregulated and 31 miRNAs were downregulated (Table I). According to the GO analysis, 'response to wounding' and 'inflammatory response' were among the top-10 altered pathways (Table II). miRNA-mRNA integrated analysis identified

Table I. Altered miRNAs in the Lass2-KO mouse liver tissues compared to the WT mouse liver tissues.

| Upregulated miRNAs | Downregulated miRNAs | |
|---|---|---|
| mmu-miR-1198-5p | mmu-miR-1192 | mmu-miR-467d-3p |
| mmu-miR-125b-5p | mmu-miR-1224-5p | mmu-miR-467f |
| mmu-miR-142-3p | mmu-miR-1247-3p | mmu-miR-483-5p |
| mmu-miR-199a-3p | mmu-miR-149-3p | mmu-miR-494-3p |
| mmu-miR-199b-3p | mmu-miR-1894-3p | mmu-miR-5109 |
| mmu-miR-199a-5p | mmu-miR-1931 | mmu-miR-5136 |
| mmu-miR-199b-5p | mmu-miR-1934-3p | mmu-miR-669a-3p |
| mmu-miR-2137 | mmu-miR-30c-1-3p | mmu-miR-669o-3p |
| mmu-miR-2861 | mmu-miR-320-3p | mmu-miR-669c-3p |
| mmu-miR-326-5p | mmu-miR-346-3p | mmu-miR-669p-3p |
| mmu-miR-34a-5p | mmu-miR-466f-3p | **mmu-miR-694** |
| mmu-miR-491-3p | mmu-miR-466h-3p | mmu-miR-711 |
| mmu-miR-5130 | mmu-miR-466i-3p | mmu-miR-744-5p |
| | mmu-miR-466q | mmu-miR-762 |
| | mmu-miR-467b-3p | mmu-miR-882 |
| | | mmu-miR-92a-2-5p |

Table II. Top 10 enrichment pathway terms from the Gene Ontology (GO) analysis (biological process).

| Gene set name | Genes in overlap | P-value |
|---|---|---|
| Response to wounding | 10 | 0.0407 |
| Humoral immune response | 3 | 0.0588 |
| Homeostasis of number of cells | 2 | 0.112 |
| Viral genome replication | 2 | 0.122 |
| Locomotory behavior | 5 | 0.122 |
| Inflammatory response | 6 | 0.148 |
| Development of primary sexual characteristics | 2 | 0.172 |
| Response to external stimulus | 12 | 0.172 |
| Jak-Stat cascade | 2 | 0.225 |
| Viral infectious cycle | 2 | 0.235 |

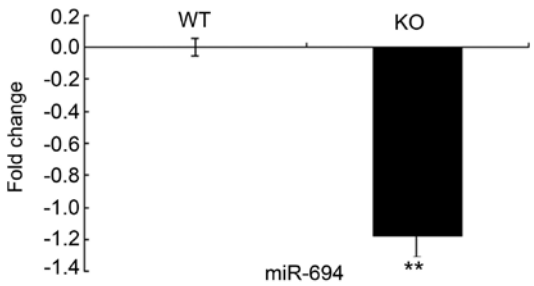


Figure 3. qPCR confirmed that miR-694 was markedly downregulated. The level of miR-694 was downregulated in the Lass2-KO liver tissues, as confirmed by qPCR. WT, wild-type; KO, knockout. **P≤0.01.

4 upregulated and 3 downregulated miRNAs and their respective negatively controlled target genes (Table III).

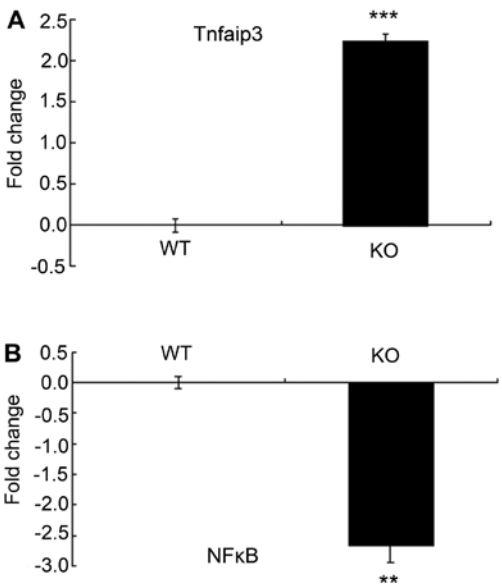


Figure 4. Tnfaip3 was markedly upregulated and NF-κB was downregulated in the Lass2-KO liver tissues. (A) qPCR assay showed that the mRNA level of Tnfaip3 was markedly upregulated. (B) mRNA level of NF-κB, which is commonly considered to be negatively regulated by Tnfaip3, was found to be downregulated. **P≤0.01 and ***P≤0.001.

*qPCR confirms that miR-694 is markedly downregulated*. The level of miR-694 was downregulated in the Lass2-KO liver tissue, as confirmed by qPCR (Fig. 3).

*Tnfaip3 is markedly upregulated whereas NF-κB is downregulated*. Tnfaip3, one of the markedly upregulated mRNAs in the Lass2-KO liver tissues, which is also a putative target gene of miR-694, was confirmed by qPCR (Fig. 4A). Its negatively controlled NF-κB was found to be downregulated (Fig. 4B).

Table III. miRNA-mRNA integrated analysis of the Lass2-KO mouse liver tissues.

A, Upregulated miRNAs and their downregulated predicted target genes

| mmu-miR-2861 | mmu-miR-5130 | mmu-miR-142-3p | mmu-miR-125b-5p |
|---|---|---|---|
| Lrrc41 | Osbpl7 | Atp2a2 | Fam116a |
| Srm | | Baz1a | Ier3ip1 |
| | | Rras | Map2k7 |
| | | Mastl | Fam78b |
| | | Arl15 | Slc17a7 |
| | | Lifr | Rasal2 |
| | | Tgfb2 | |
| | | Myst2 | |

B, Downregulated miRNAs and their upregulated predicted target genes

| mmu-miR-1192 | mmu-miR-466f-3p | | **mmu-miR-694** |
|---|---|---|---|
| Tcf4 | Pgm2l1 | Col4a1 | Mef2c |
| Ap3m1 | Tm6sf1 | Junb | Ncoa7 |
| Sgk1 | Angptl2 | Cttnbp2nl | Ska1 |
| Scd2 | Prc1 | 2700081O15Rik | Gng2 |
| Adam23 | Smad7 | Ptgfrn | Abi2 |
| Elavl4 | Klf6 | Ncoa7 | Nipal1 |
| Rbm28 | Trp53inp1 | Zfp532 | **Tnfaip3** |
| Phf15 | Tmem65 | Samd4 | Fam120c |
| Arrdc4 | Dgkd | Prrg3 | Srebf1 |
| Slc16a5 | Fam120c | Zmat3 | Man1c1 |
| Arhgef17 | Gpm6b | Ptp4a1 | Vldlr |
| Zfp532 | Nr4a1 | Adam23 | Fbln5 |
| Nrxn2 | Eif4enif1 | Tcf4 | Rai2 |
| Ccna2 | Mef2c | Jun | Prrg3 |
| | Fam46a | Pde4d | Fam46a |
| | Elavl4 | Tnfaip8 | Plekha6 |
| | Odz3 | | E130203B14Rik |
| | | | Nup153 |
| | | | Trib1 |
| | | | Cd63 |
| | | | Pde5a |
| | | | Serpinh1 (PAI-1) |
| | | | Sgms1 |
| | | | Elavl4 |
| | | | Pde4d |

## Discussion

Lass2 is a member of the Lass family, which is conserved among eukaryotes and is abundantly distributed in the liver, kidney and brain. The major function of Lass2 is synthesizing long-chain ceramide-C:24-26 (6). Ceramide serves as the precursor of a series of more complex sphingolipids. Short-chain ceramides function as a second messenger in a variety of cellular events, including apoptosis and differentiation (7,8), and regulate various cellular processes linked to cancer development, progression, metastasis and resistance to therapy (9,10). By comparison, long-chain ceramide, as the important element in constructing membranous structures, may regulate the cellular behavior via influencing the property of membranes. For example, ablation of Lass2 causes morphological alterations of the property of membranes (11,12). In the present study, numerous vesicles were noted in the hepatocytes from young Lass2-KO mice (Fig. 1), in accordance with previous reports from other researchers. Based on the attenuated production of albumin and increased hepatic biochemical

Table IV. Functions of the miR-694 predicted target genes.

| Function | miR-694 target gene (ref.) |
|---|---|
| Transcription | Mef2c (21) |
| | Ncoa7 (22) |
| | Tnfaip3 (13,14) |
| | Elavl4 (23,24) |
| Cell cycle | Ska1 (25) |
| | Nup153 (26) |
| Cell signal transduction | Gng2 (27) |
| | Abi2 (28,29) |
| | Pde5a (30) |
| | Pde4d (31) |
| Metabolism regulator | Trib1 (32-34) |
| | Sgms1 (35-37) |
| | Srebf1 (38) |
| | Vldlr (39) |
| Trafficking | CD63 (40,41) |
| | Man1c1 (42) |
| | Nup153 (26) |
| | Sgms1 (43) |
| ECM deposition | Fbln5 (44,45) |
| | PAI-1 (46) |
| Immunity regulation | Trib1 (47,48) |
| | Tnfaip3 (13,14) |

indices in the Lass2-KO mice, (Fig. 2), it appears that the hepatocellular-specific Lass2-KO mice underwent hepatocellular injury even at an early age.

The microarrays of mRNAs and miRNAs of the Lass2-KO mice liver tissues vs. control demonstrated that miR-694 was upregulated, which was confirmed by qPCR. Moreover, the predicted target gene Tnfaip3 was found to be upregulated, as shown in the results of either the microarray of mRNA or qPCR. NF-κB, which is usually commonly negatively controlled by Tnfaip3 was found downregulated in the Lass2-KO mouse liver tissues. In our previous study (5), another target gene Serpinh1 (PAI-1) of miR-694 was found to be upregulated. The data strongly suggest that Lass2 deletion influences the expression level of miR-694.

However, the function of miR-694 is uncertain. According to miRNA-mRNA integrated analysis in this study, the downregulated Lass2-related miR-694 elevated 25 mRNAs including Tnfaip3. Tnfaip3 is commonly considered as an inflammation suppressor (13) by inactivation of lymphocytes of suppressing NF-κB (14,15). Although it is commonly considered a tumor suppressor, overexpression of Tnfaip3 has also been reported in several non-lymphoma solid cancers, including HCC (16-18). Our data suggest that Tnfaip3/NF-κB might play a role in inhibiting the inflammation and protecting injured hepatocytes caused by deletion of Lass2. In another report, Lass2-KO mice displayed resistance to LPS-induced liver injury (19), which might also be explained by the inhibitory immunity mediated by Tnfaip3/NF-κB.

The functions of other predicted target genes of miR-694 are listed in Table IV. According to published reports, miR-694 target genes are involved it the regulation of various important cellular events, including transcription, cell signal transduction, metabolism of lipid and glucose and trafficking, suggesting a diversity of regulatory functions of miR-694. miRNAs act as highly effective regulators of intracellular events. Moreover, via endocytosis or exocytosis of miRNA-containing vesicles, miRNAs modulate the extracellular milieu including stromal cells and extracellular matrix (20). For example, altered Tnfaip3/NF-κB may influence the immunocytes in the liver, or PAI-1 which was found to be upregulated, may regulate the synthesis of ECM in the liver (5), either of which is a predicted target gene of miR-694. The actual functions of miR-694 may likely be beyond what is listed in Table IV.

Overall, the present study first reports the attenuated expression level of miR-694 in Lass2-KO mouse liver tissue and its alteration of the Tnfaip3/NF-κB pathway. Our data strongly suggest that miR-694 functions in maintaining homeostasis of the liver and provide the basis to explore the functions of Lass2-related microRNAs.

## Acknowledgements

This study was supported by the Grant from the State Key Laboratory of Oncogenes and Related Genes (no. 90-10-02, to X.L.) and Clinical Medicine Science & Technology Project of Jiangsu Province of China (no. BL2013024).

## References

1. Pewzner-Jung Y, Ben-Dor S and Futerman AH: When do Lasses (longevity assurance genes) become CerS (ceramide synthases)? Insights into the regulation of ceramide synthesis. J Biol Chem 281: 25001-25005, 2006.
2. Wang H, Wang J, Zuo Y, *et al*: Expression and prognostic significance of a new tumor metastasis suppressor gene LASS2 in human bladder carcinoma. Med Oncol 29: 1921-1927, 2012.
3. Fan S, Niu Y, Tan N, *et al*: LASS2 enhances chemosensitivity of breast cancer by counteracting acidic tumor microenvironment through inhibiting activity of V-ATPase proton pump. Oncogene 32: 1682-1690, 2013.
4. Imgrund S, Hartmann D, Farwanah H, *et al*: Adult ceramide synthase 2 (CERS2)-deficient mice exhibit myelin sheath defects, cerebellar degeneration, and hepatocarcinomas. J Biol Chem 284: 33549-33560, 2009.
5. Chen L, Lu X, Zeng T, *et al*: Enhancement of DEN-induced liver tumourigenesis in hepatocyte-specific Lass2-knockout mice coincident with upregulation of the TGF-β1-Smad4-PAI-1 axis. Oncol Rep 31: 885-893, 2014.
6. Teufel A, Maass T, Galle PR, *et al*: The longevity assurance homologue of yeast lag1 (Lass) gene family (Review). Int J Mol Med 23: 135-140, 2009.
7. Morad SAF and Cabot MC: Ceramide-orchestrated signalling in cancer cells. Nat Rev Cancer 13: 51-65, 2013.
8. Stiban J, Tidhar R and Futerman AH: Ceramide synthases: roles in cell physiology and signaling. Adv Exp Med Biol 688: 60-71, 2010.
9. Saddoughi SA and Ogretmen B: Diverse functions of ceramide in cancer cell death and proliferation. Adv Cancer Res 117: 37-58, 2010.
10. Liu J, Beckman BS and Foroozesh M: A review of ceramide analogs as potential anticancer agents. Future Med Chem 5: 1405-1421, 2013.
11. Park JW, Park WJ, Kuperman Y, Boura-Halfon S, Pewzner-Jung Y and Futerman AH: Ablation of very long acyl chain sphingolipids causes hepatic insulin resistance in mice due to altered detergent-resistant membranes. Hepatology 57: 525-532, 2013.
12. Silva LC, Ben David O, Pewzner-Jung Y, *et al*: Ablation of ceramide synthase 2 strongly affects biophysical properties of membranes. J Lipid Res 53: 430-436, 2012.

13. Ma A and Malynn BA: A20: linking a complex regulator of ubiquitylation to immunity and human disease. Nat Rev Immunol 12: 774-785, 2012.
14. Pujari R, Hunte R, Khan W and Shembade N: A20-mediated negative regulation of canonical NF-κB signaling pathway. Immunol Res 57: 166-171, 2013.
15. Zhang F, Yang L and Li Y: The role of A20 in the pathogenesis of lymphocytic malignancy. Cancer Cell Int 12: 44, 2012.
16. Wang M and Li S: Bladder polypoid cystitis-derived A20 associates with tumorigenesis. Cell Biochem Biophys 67: 669-673, 2013.
17. Hjelmeland AB, Wu Q, Wickman S, *et al*: Targeting A20 decreases glioma stem cell survival and tumor growth. PLoS Biol 8: e1000319, 2010.
18. Wang CM, Wang Y, Fan CG, *et al*: miR-29c targets TNFAIP3, inhibits cell proliferation and induces apoptosis in hepatitis B virus-related hepatocellular carcinoma. Biochem Biophys Res Commun 411: 586-592, 2011.
19. Ali M, Fritsch J, Zigdon H, Pewzner-Jung Y, Schütze S and Futerman AH: Altering the sphingolipid acyl chain composition prevents LPS/GLN-mediated hepatic failure in mice by disrupting TNFR1 internalization. Cell Death Dis 4: e929, 2013.
20. Su Y, Li X, Ji W, *et al*: Small molecule with big role: MicroRNAs in cancer metastatic microenvironments. Cancer Lett 344: 147-156, 2014.
21. Cante-Barrett K, Pieters R and Meijerink JPP: Myocyte enhancer factor 2C in hematopoiesis and leukemia. Oncogene 33: 403-410, 2014.
22. Higginbotham KS, Breyer JP, Bradley KM, *et al*: A multistage association study identifies a breast cancer genetic locus at NCOA7. Cancer Res 71: 3881-3888, 2011.
23. Bronicki LM and Jasmin BJ: Emerging complexity of the HuD/ELAVl4 gene; implications for neuronal development, function, and dysfunction. RNA 19: 1019-1037, 2013.
24. Lee EK, Kim W, Tominaga K, *et al*: RNA-binding protein HuD controls insulin translation. Mol Cell 45: 826-835, 2012.
25. Ye AA and Maresca TJ: Cell division: kinetochores SKAdaddle. Curr Biol 23: R122-R124, 2013.
26. Ullman KS, Shah S, Powers MA and Forbes DJ: The nucleoporin nup153 plays a critical role in multiple types of nuclear export. Mol Biol Cell 10: 649-664, 1999.
27. Matsuda T, Hashimoto Y, Ueda H, *et al*: Specific isoprenyl group linked to transducin gamma-subunit is a determinant of its unique signaling properties among G-proteins. Biochemistry 37: 9843-9850, 1998.
28. Grove M, Demyanenko G, Echarri A, *et al*: ABI2-deficient mice exhibit defective cell migration, aberrant dendritic spine morphogenesis, and deficits in learning and memory. Mol Cell Biol 24: 10905-10922, 2004.
29. Dai Z and Pendergast AM: Abi-2, a novel SH3-containing protein interacts with the c-Abl tyrosine kinase and modulates c-Abl transforming activity. Genes Dev 9: 2569-2582, 1995.
30. Kulkarni SK and Patil CS: Phosphodiesterase 5 enzyme and its inhibitors: update on pharmacological and therapeutical aspects. Methods Find Exp Clin Pharmacol 26: 789-799, 2004.
31. Lynch MJ, Baillie GS and Houslay MD: cAMP-specific phosphodiesterase-4D5 (PDE4D5) provides a paradigm for understanding the unique non-redundant roles that PDE4 isoforms play in shaping compartmentalized cAMP cell signalling. Biochem Soc Trans 35: 938-941, 2007.
32. Ishizuka Y, Nakayama K, Ogawa A, *et al*: TRIB1 downregulates hepatic lipogenesis and glycogenesis via multiple molecular interactions. J Mol Endocrinol 52: 145-158, 2014.
33. Angyal A and Kiss-Toth E: The tribbles gene family and lipoprotein metabolism. Curr Opin Lipidol 23: 122-126, 2012.
34. Dugast E, Kiss-Toth E, Soulillou JP, Brouard S and Ashton-Chess J: The Tribbles-1 protein in humans: roles and functions in health and disease. Curr Mol Med 13: 80-85, 2013.
35. Vacaru AM, Tafesse FG, Ternes P, *et al*: Sphingomyelin synthase-related protein SMSr controls ceramide homeostasis in the ER. J Cell Biol 185: 1013-1027, 2009.
36. Liu J, Zhang H, Li Z, *et al*: Sphingomyelin synthase 2 is one of the determinants for plasma and liver sphingomyelin levels in mice. Arterioscler Thromb Vasc Biol 29: 850-856, 2009.
37. Separovic D, Hanada K, Awad Maitah MIY, *et al*: Sphingomyelin synthase 1 suppresses ceramide production and apoptosis post-photodamage. Biochem Biophys Res Commun 358: 196-202, 2007.
38. Ruiz R, Jideonwo V, Ahn M, *et al*: Sterol regulatory element-binding protein-1 (SREBP-1) is required to regulate glycogen synthesis and gluconeogenic gene expression in mouse liver. J Biol Chem 289: 5510-5517, 2014.
39. Go GW and Mani A: Low-density lipoprotein receptor (LDLR) family orchestrates cholesterol homeostasis. Yale J Biol Med 85: 19-28, 2012.
40. Pols MS and Klumperman J: Trafficking and function of the tetraspanin CD63. Exp Cell Res 315: 1584-1592, 2009.
41. Maecker HT, Todd SC and Levy S: The tetraspanin superfamily: molecular facilitators. FASEB J 11: 428-442, 1997.
42. Scott DW and Patel RP: Endothelial heterogeneity and adhesion molecules N-glycosylation: implications in leukocyte trafficking in inflammation. Glycobiology 23: 622-633, 2013.
43. Subathra M, Qureshi A and Luberto C: Sphingomyelin synthases regulate protein trafficking and secretion. PLoS One 6: e23644, 2011.
44. Kapustin A, Stepanova V, Aniol N, *et al*: Fibulin-5 binds urokinase-type plasminogen activator and mediates urokinase-stimulated β1-integrin-dependent cell migration. Biochem J 443: 491-503, 2012.
45. Choi J, Bergdahl A, Zheng Q, Starcher B, Yanagisawa H and Davis EC: Analysis of dermal elastic fibers in the absence of fibulin-5 reveals potential roles for fibulin-5 in elastic fiber assembly. Matrix Biol 28: 211-220, 2009.
46. Declerck PJ and Gils A: Three decades of research on plasminogen activator inhibitor-1: a multifaceted serpin. Semin Thromb Hemost 39: 356-364, 2013.
47. Satoh T, Kidoya H, Naito H, *et al*: Critical role of Trib1 in differentiation of tissue-resident M2-like macrophages. Nature 495: 524-528, 2013.
48. Dugast E, Kiss-Toth E, Docherty L, *et al*: Identification of Tribbles-1 as a novel binding partner of Foxp3 in regulatory T cells. J Biol Chem 288: 10051-10060, 2013.